Intermetallic Reactions in Reflowed and Aged Sn-9Zn Solder Ball Grid Array Packages with Au/Ni/Cu and Ag/Cu Pads

HSIU-JEN LIN[1] and TUNG-HAN CHUANG[1,2]

1.—Institute of Materials Science and Engineering, National Taiwan University, Taipei 106, Taiwan. 2.—E-mail: tunghan@ccms.ntu.edu.tw

During the reflowing of Sn-9Zn solder ball grid array (BGA) packages with Au/Ni/Cu and Ag/Cu pads, the surface-finished Au and Ag film dissolved rapidly and reacted with the Sn-9Zn solder to form a γ_3-$AuZn_4$/γ-Au_7Zn_{18} intermetallic double layer and ε-$AgZn_6$ intermetallic scallops, respectively. The growth of γ_3-$AuZn_4$ is prompted by further aging at 100°C through the reaction of γ-Au_7Zn_{18} with the Zn atoms dissolved from the Zn-rich precipitates embedded in the β-Sn matrix of Sn-9Zn solder BGA with Au/Ni/Cu pads. No intermetallic compounds can be observed at the solder/pad interface of the Sn-9Zn BGA specimens aged at 100°C. However, after aging at 150°C, a Ni_4Zn_{21} intermetallic layer is formed at the interface between Sn-9Zn solder and Ni/Cu pads. Aging the immersion Ag packages at 100°C and 150°C caused a γ-Cu_5Zn_8 intermetallic layer to appear between ε-$AgZn_6$ intermetallics and the Cu pad. The scallop-shaped ε-$AgZn_6$ intermetallics were found to detach from the γ-Cu_5Zn_8 layer and float into the solder ball. Accompanied with the intermetallic reactions during the aging process of reflowed Sn-9Zn solder BGA packages with Au/Ni/Cu and Ag/Cu pads, their ball shear strengths degrade from 8.6 N and 4.8 N to about 7.2 N and 2.9 N, respectively.

Key words: Intermetallic compounds, Sn-9Zn, Au/Ni/Cu pads, Ag/Cu pads, ball shear strength

INTRODUCTION

Out of environmental concerns, the development of Pb-free solders has become a key issue for the electronics industry. Compared to many other promising Pb-free solders, such as Sn3.5Ag, Sn0.7Cu, and Sn-Ag-Cu, eutectic Sn-9Zn has the merits of a lower melting point (199°C) and better cost performance.[1] However, further research efforts are required to address its disadvantages, such as poor wettability and oxidation resistance, so that the improvements made on eutectic Sn-9Zn can facilitate the development of an actual replacement for Sn-Pb solders. In addition, the reliability of Sn-9Zn solder joints on various surface-finished pads for electronic packaging should also be evaluated.

The Au/Ni surface finish has been widely used for printed circuit boards to protect Cu pads from oxidation and promote the wettability of liquid solder.[2] During the reflow process, the Au thin film dissolves rapidly into the solder matrix, triggering the occurrence of further interfacial reaction between the solder and the Ni substrate. In the cases of traditional Sn-Pb solders and most Pb-free solders (such as Sn-Ag, Sn-Cu, and Sn-Bi), their reactions with Ni substrates lead to the formation of Ni_3Sn_4 intermetallic compounds.[3–5] However, a liquid Sn-Zn solder alloy reacts with Ni to form $Ni_{19.0}Zn_{80.0}Sn_{1.0}$ intermetallics due to the high activity of the element Zn.[6] A soldering reaction between liquid Sn-8Zn-3Bi and Ni substrate was reported to result in a continuous intermetallic layer of Ni_5Zn_{21} at temperatures below 325°C and a double layer of Ni_5Zn_{21}/$Ni_{35}Zn_{22}Sn_{43}$ at above 325°C.[7] Harris also showed that a solid/solid interfacial reaction between Sn-Zn-Bi solder and Ni substrate at 125°C for 100 days caused the formation of a Ni-85.9wt.%Zn intermetallic compound.[8] In addition, Shiue et al. aged a series of Sn-Zn based solders joined with Au/Ni-P/Cu substrates and reported an intermetallic compound of Zn-rich γ phase ($NiZn_3$) at the interface.[9]

For the Pb-free BGA packages with Au/Ni/Cu

(Received May 2, 2005; accepted August 30, 2005)

pads, various failures such as Au embrittlement and black pads have been reported.[2] In addition, the Au/Ni electro- or electroless-plating process is quite costly and complex. Immersion silver is an effective alternative method for the surface finishing of Cu pads. The process involving immersion Ag takes about 7 min, and the cost is close to that of processes involving traditional Sn.[3] Immersion Ag can provide smooth surfaces and good wettability for liquid solders on Cu pads. During reflow, the Ag metallization (about 0.2 μm in thickness) also dissolves rapidly into the solder matrix, causing the intermetallic reactions at the interfaces between the solder alloy and the Cu pads.

For the interfacial reactions of Sn-Pb solders and most Pb-free solders with Cu pads, Cu_6Sn_5 and Cu_3Sn intermetallic compounds have also been reported.[10] However, a Sn-Zn/Cu interfacial reaction was reported to generate Cu-Zn intermetallics on account of the high activity of the element Zn. Chan et al. studied the soldering reactions between liquid Sn-9Zn and Cu substrates and found $Cu_{33.4}Zn_{66.5}Sn_{0.1}$ at the interfaces.[11] Suganuma et al. also investigated the soldering reactions between liquid Sn-Zn and Cu substrates at temperatures ranging from 230°C to 280°C for 5–35 min.[12] Three layers of interfacial intermetallic compounds (γ-Cu_5Zn_8, β'-CuZn, and an unknown thin-layer phase) were found. The total thickness of these intermetallics increased with the increasing Zn content in the Sn-Zn solders. Lin and Chuang further analyzed the intermetallic reactions between liquid Sn-8Zn-3Bi solder and Cu substrates in a wide temperature range of 225–350°C for 30–90 min.[13] The results indicated that a planar layer of $Cu_{32.1}Zn_{66.7}Sn_{0.7}Bi_{0.5}$ (γ phase) along with a great number of scallop-shaped intermetallic compounds of $Cu_{19.3}Zn_{77.8}Sn_{2.9}$ (ε phase) appeared at the interfaces at temperatures below 325°C. At temperatures higher than 325°C, the ε-intermetallic scallops disappeared, and the planar γ-intermetallics became cluster shaped. For the solid/solid interfacial reactions between various Sn-Zn solders and Cu substrates, Lee et al.[14] and Yoon et al.[15,16] reported a γ-Cu_5Zn_8 intermetallic compound after aging at 100°C, 130°C, and 160°C. In addition, Harris showed that 13-μm-thick γ-Cu_5Zn_8 intermetallics appeared at the Sn-Zn-Bi/Cu interface after aging at 125°C for 100 days.[8] This study focused on the intermetallic reactions and related bonding strengths of the eutectic Sn-9Zn solder joints in a ball grid array (BGA) package with Au/Ni/Cu and Ag/Cu pads after the reflow and aging processes.

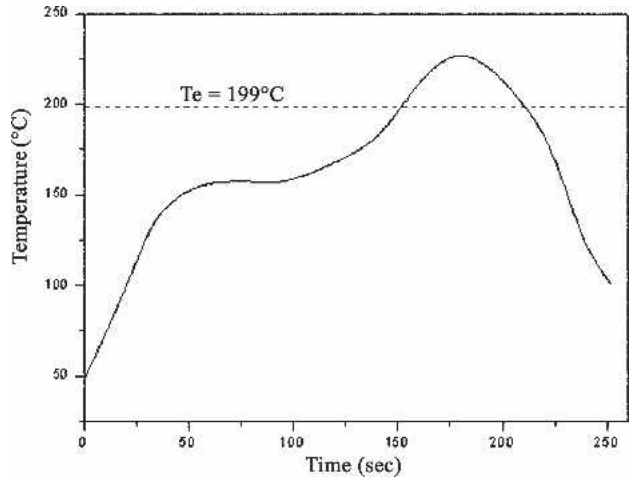

Fig. 1. Temperature profile of the reflow process for Sn-9Zn solder BGA packages in this study with Au/Ni/Cu and Ag/Cu pads.

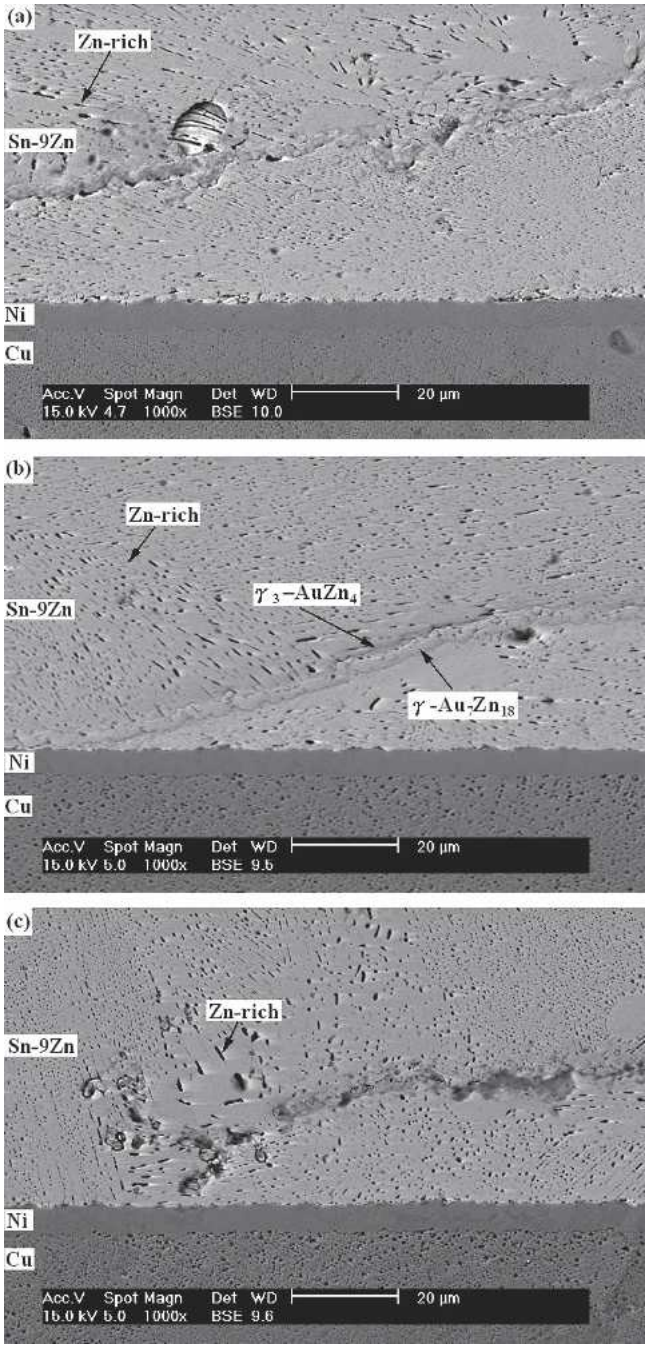

Fig. 2. Morphology of the floating intermetallic layers in Sn-9Zn solder BGA packages with Au/Ni/Cu pads after multiple reflows: (a) one time, (b) two times, and (c) three times.

EXPERIMENTAL PROCEDURE

Ball grid array packages with Au/Ni/Cu pads were electroplated with a 5-μm-thick layer of Ni and immersion plated with a 0.5-μm-thick layer of Au, while those with Ag/Cu pads were immersion deposited with a 0.2-μm-thick layer of Ag. Sn-9Zn (wt.%) solder balls of 0.4 mm in diameter were dipped in rosin mildly activated (RMA) flux, placed on the Au/Ni and Ag surface finished Cu pads, and then reflowed in a hot air furnace equipped with five heating zones. Figure 1 shows the temperature profile adopted for the reflow process. During reflow, liquid Sn-9Zn solder reacted with Au/Ni/Cu and Ag/Cu pads to form intermetallic compounds at the interfaces.

For further evaluation of the intermetallic reactions in Sn-9Zn BGA packages as electronic devices were in operation and the solder joints were being heated, certain reflowed specimens were aged at 100°C and 150°C for various time periods, and a solid/solid reaction was observed to occur at the solder/pad interface under this condition.

The BGA packages, after reflow and aging, were cross-sectioned through a row of Sn-9Zn solder balls. They were then cold-mounted, ground with 1500 grit SiC paper, and polished with 0.3-μm alumina powder. The morphology and chemical composition of intermetallic compounds were analyzed using a scanning electron microscope equipped with energy-dispersive x-ray spectrometry (EDX). Finally, ball shear tests were conducted to measure the bonding strengths of the solder joints. For this purpose, a shear rate of 0.1 mm/s and a shear height of 80 μm (about 1/4 the reflowed ball height) were employed.

RESULTS AND DISCUSSION

The microstructure of the Sn9Zn solder BGA packages with Au/Ni/Cu pads after multiple reflows is shown in Fig. 2. The solder matrix contains many needle-shape Zn-rich precipitates embedded in the β-Sn matrix. The Zn content in the β-Sn matrix, as analyzed by EDX, is 2.2 wt.% (4 at.%). During the reflow process, the Au thin film on Au/Ni/Cu pads dissolves rapidly, and the resultant intermetallic compounds that are formed at the solder/pad interfaces take the appearance of a planar double layer. The intermetallic layer tends to float away from the interfaces even after the first reflow (Fig. 2). Increasing the reflow cycles causes the intermetallic compounds to float farther away. The composition (at.%) of the inner layer of the intermetallics, as analyzed by EDX, is Au:Zn = 28.9:71.1, which corresponds to the γ phase (Au_7Zn_{18}) in the Au-Zn equilibrium diagram. The outer intermetallic layer has a higher Zn content (Au:Zn = 18.7:81.3), which corresponds to the γ_3 phase ($AuZn_4$) in the Au-Zn equilibrium diagram. The microstructure of the Sn-9Zn

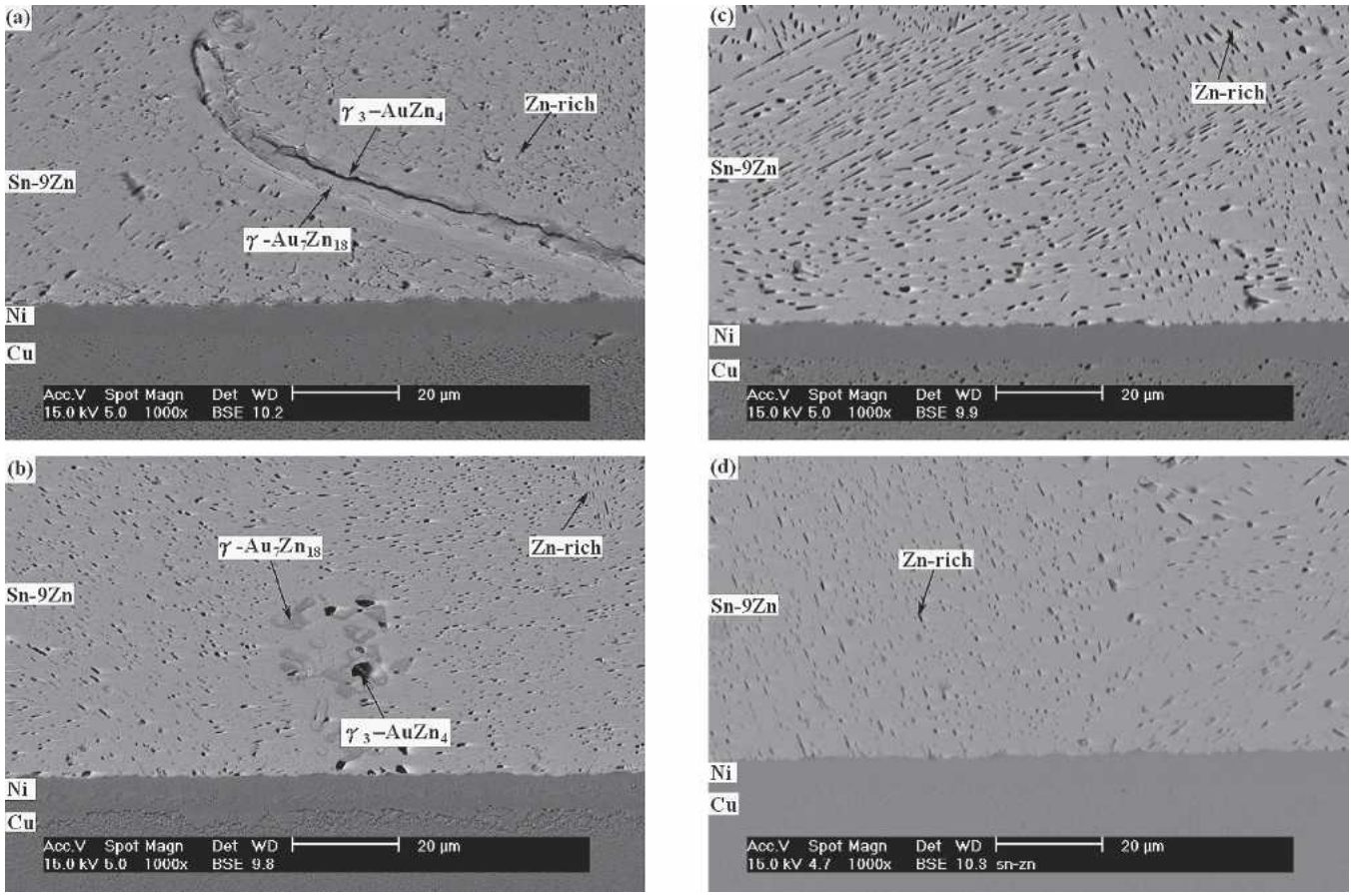

Fig. 3. Microstructure of the Sn-9Zn solder joints in BGA packages with Au/Ni/Cu pads after aging at 100°C for various times: (a) 100 h, (b) 500 h, (c) 700 h, and (d) 1000 h.

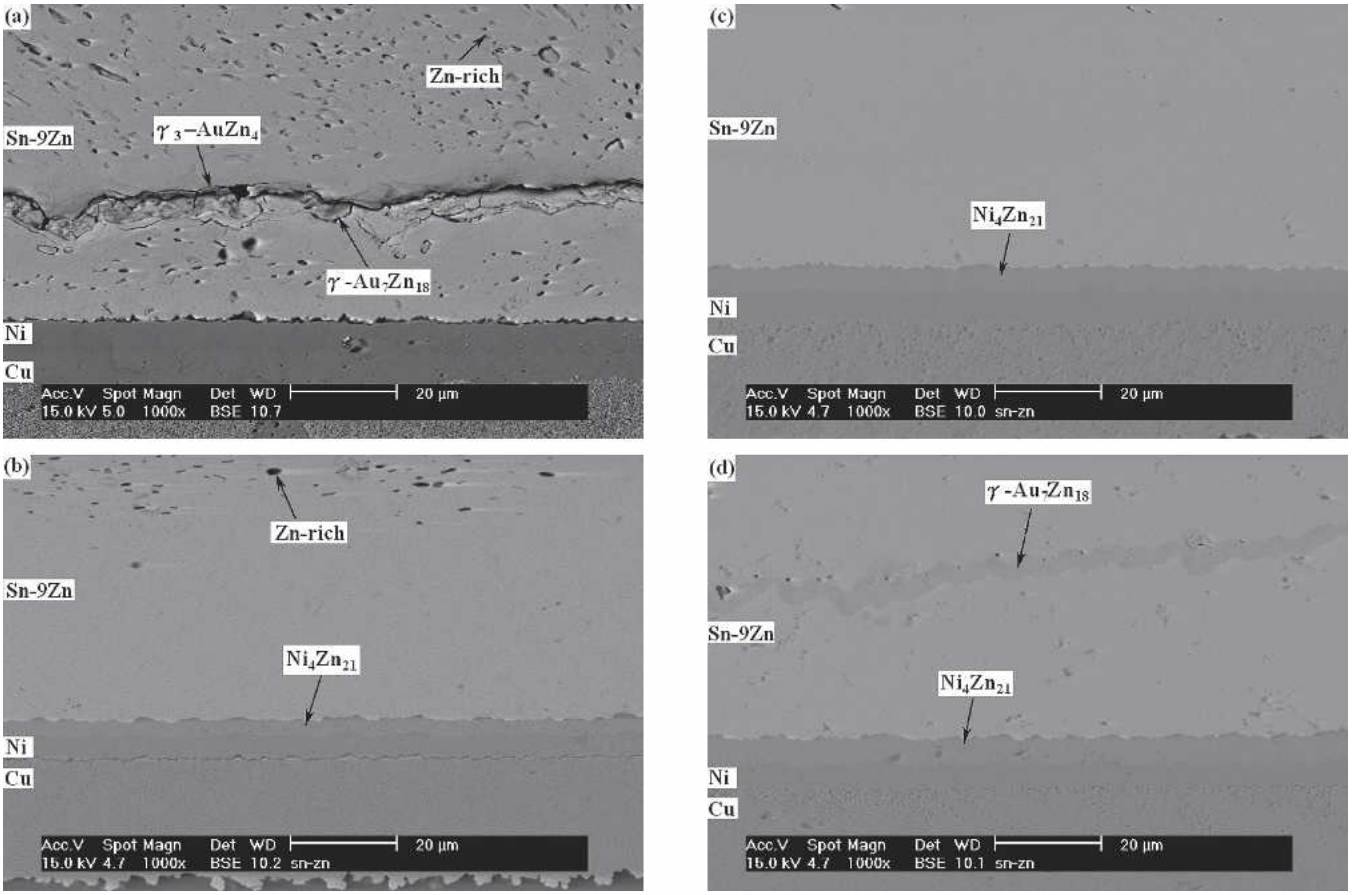

Fig. 4. Microstructure of the Sn-9Zn solder joints in BGA packages with Au/Ni/Cu pads after aging at 150°C for various times: (a) 100 h, (b) 500 h, (c) 700 h, and (d) 1000 h.

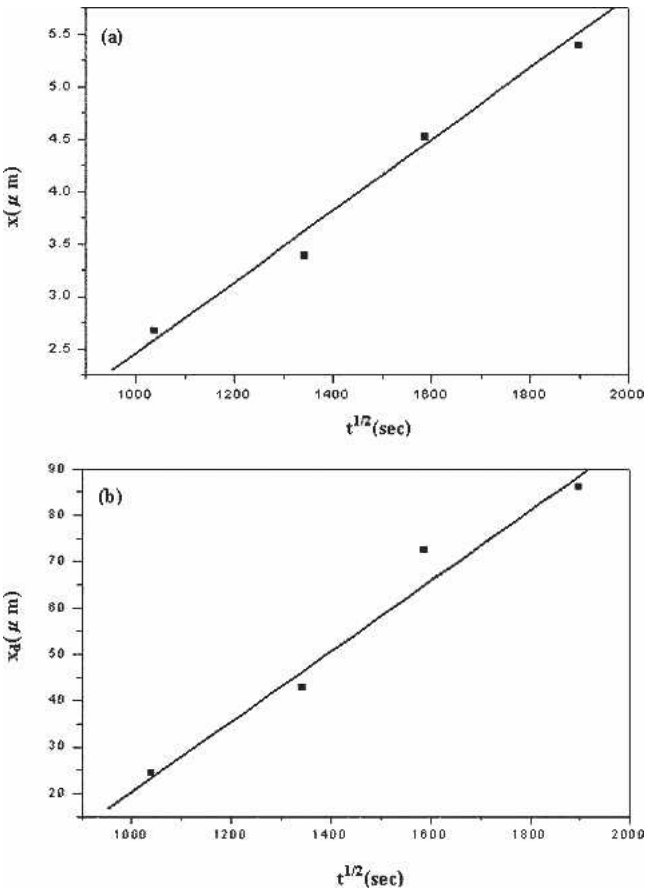

Fig. 5. Thickness (x) of the Ni_4Zn_{21} interfacial intermetallic layer and precipitate-free zone (x_d) in the solder matrix of Au/Ni surface finished Sn-9Zn BGA packages after aging at 150°C relative to the square root of time ($t^{1/2}$).

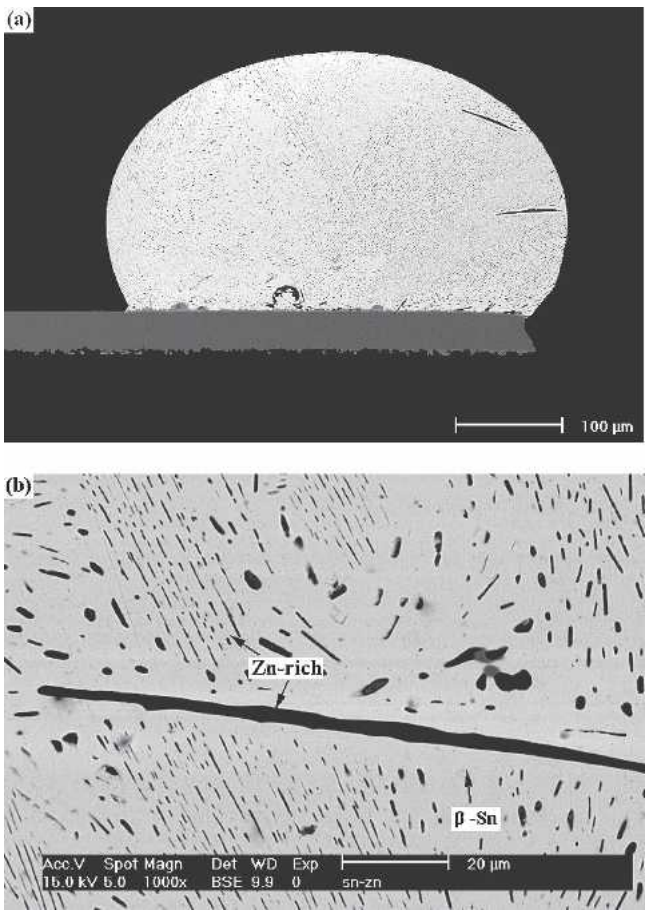

Fig. 6. Morphology of (a) the as-reflowed Sn-9Zn solder ball with Ag/Cu and (b) the microstructure of the as-reflowed Sn-9Zn matrix.

solder joints remains unchanged after aging at 100°C, as evidenced by Fig. 3. However, the γ_3-$AuZn_4$ intermetallic layer grows with the diminishing of γ-Au_7Zn_{18} as the aging time increases, and the Zn content in the β-Sn matrix increases slightly to 2.3 wt.% (4.2 at.%). Following the floating away of the γ_3/γ intermetallic layer, no further intermetallic reaction can be observed at the interface between the Sn-9Zn solder and the Ni/Cu pad even after a prolonged aging time of 1000 h.

However, aging at 150°C causes a planar intermetallic phase to form at the solder/pad interface of Au/Ni surface finished Sn-9Zn BGA packages, as shown in Fig. 4. The EDX analysis indicates that the composition (at.%) of these interfacial intermetallics is Ni:Zn = 16.1:83.9, which corresponds to the Ni_4Zn_{21} phase; also, the Zn content in the β-Sn matrix is increased slightly further to 2.4 wt.% (4.3 at.%). Figure 4 reveals that the Ni_4Zn_{21} intermetallic layer grows with the increase in aging time at 150°C. The thickness of the Ni_4Zn_{21} intermetallic layer is measured and plotted against the square root of aging time ($t^{1/2}$), as shown by Fig. 5a, where the linear relation of the curve indicates that the intermetallic growth is diffusion controlled. Figure 4 also indicates that the growth of Ni_4Zn_{21} intermetallic compounds causes the depletion of Zn-rich precipitates in the solder balls near the Ni/Cu pads. The result indicates that the Ni_4Zn_{21} intermetallics are formed through the interfacial reaction of the Ni layer with the Zn atoms from the solder matrix. The consumption of Zn content in the Sn-9Zn solder caused the dissolution of Zn-rich precipitates near the solder/pad interfaces. Figure 5b shows that the thickness of precipitation-free zones increases parabolically with the aging time, giving the implication that the reaction is diffusion controlled. The lattice diffusivity of Zn in the Sn matrix at 150°C, as calculated from the equation of Huang and Huntington,[17]

$$D\ (m^2/s) = 1.1 \times 10^{-6} \exp\left(-\frac{50.2\ kJ/mol}{RT}\right),$$

is 6.91×10^{-13} m^2/s. The diffusion distances $d = (\sqrt{Dt})$ at this temperature for 100 h and 1000 h are 499 μm and 1577 μm, respectively. In comparison with Fig. 6, it is evidenced that the depletion thicknesses of Zn-rich precipitates after aging at 150°C for durations of 100 h to 1000 h are about 15-fold smaller than the diffusion distances of Zn atoms in the Sn matrix. The results indicate that the kinetics-controlled mechanism for the dissolution of Zn-rich precipitates in the Au/Ni surface finished Sn-9Zn BGA packages is the interfacial reaction between Sn-9Zn solder and the Ni film on Cu pads, rather than the lattice diffusion of Zn atoms through the solder matrix.

The microstructure of the as-reflowed Sn-9Zn solder ball in a BGA package with Ag/Cu pads, as shown in Fig. 6, also consists of many needlelike Zn-rich precipitates embedded in the Sn-rich matrix. However, in addition to those fine precipitates, a small number of coarsened Zn-rich plates also appear in the immersion Ag surface finished Sn-9Zn solder BGA packages. Figure 7 shows that the coarsened Zn-rich plates display a much greater tendency to form near the as-reflowed solder/pad interface. Those fine precipitates are found to diminish around the coarsened Zn-rich plates. The reflow process also leads to the formation of a thin layer of scallop-shaped intermetallic compounds at the interface of the solder joints. The chemical composition (at.%) of these interfacial intermetallics, as analyzed by EDX,

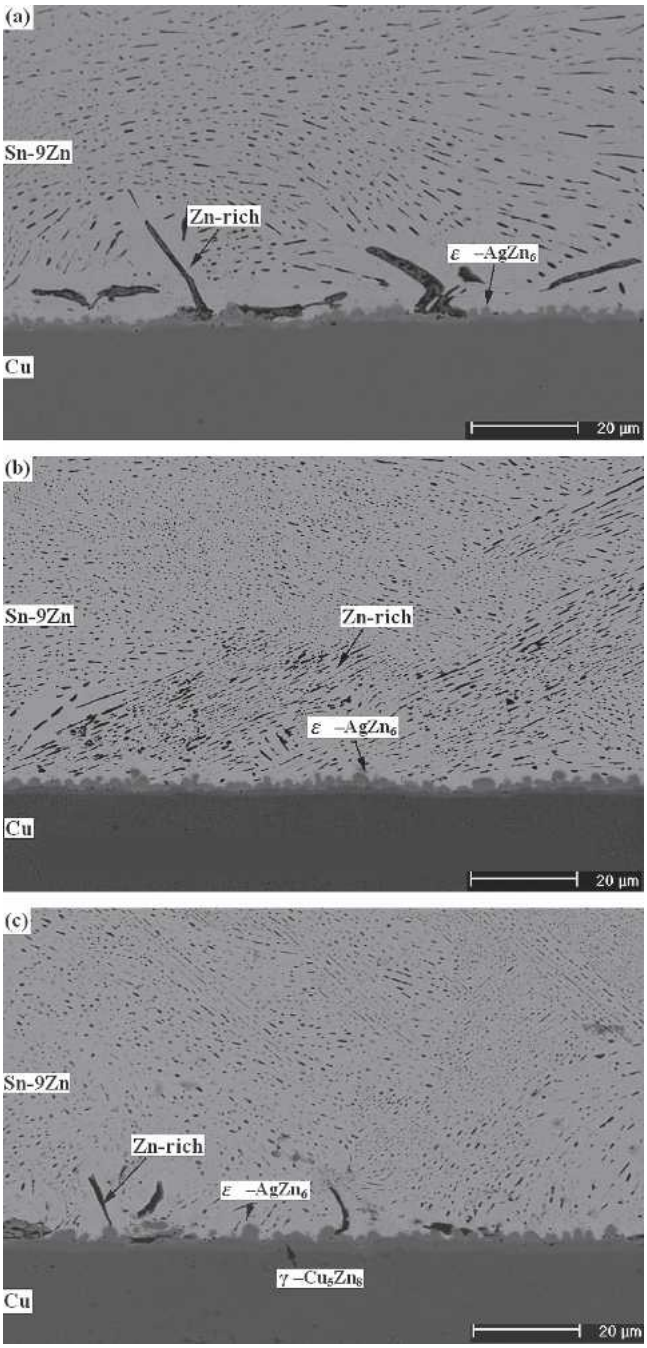

Fig. 7. Morphology of the intermetallic compounds formed at the interface of Sn-9Zn solder BGA packages with Ag/Cu pads after multiple reflows: (a) one time, (b) two times, and (c) three times.

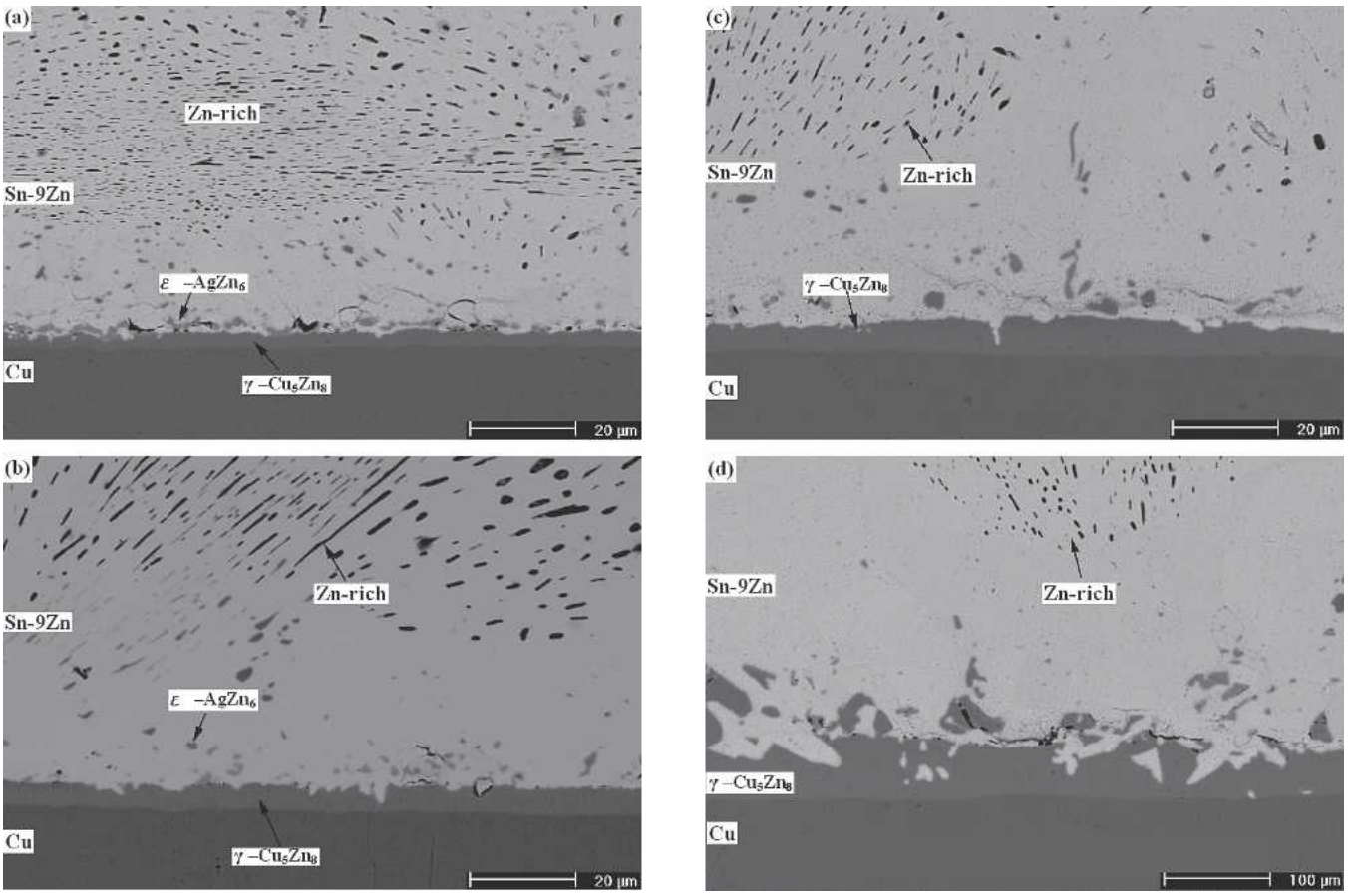

Fig. 8. Microstructure of intermetallic compounds formed in the Sn-9Zn solder BGA packages with Ag/Cu pads after aging at 100°C for various time periods: (a) 100 h, (b) 300 h, (c) 700 h, and (d) 1000 h.

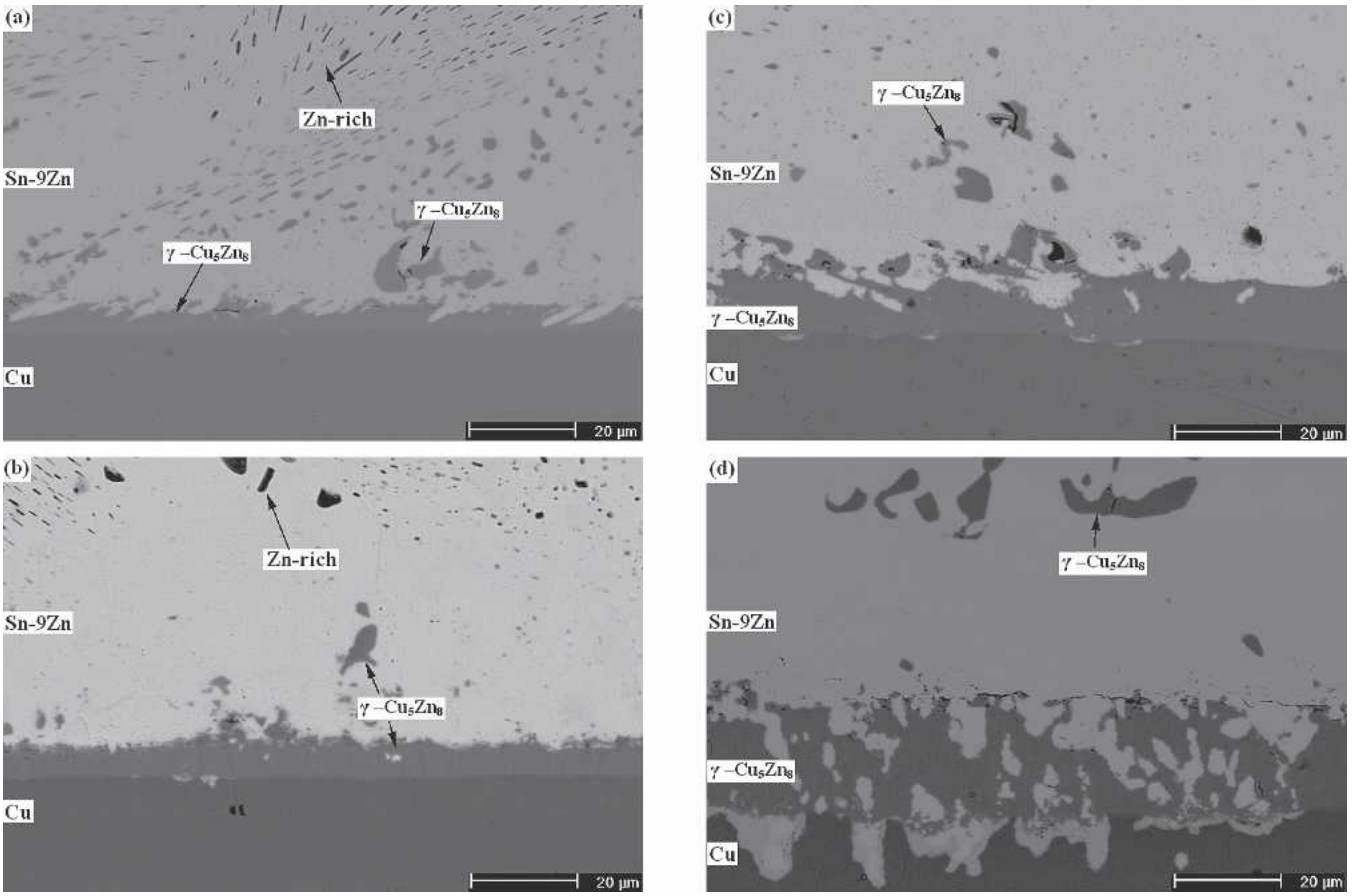

Fig. 9. Microstructure of intermetallic compounds formed in the Sn-9Zn solder BGA packages with Ag/Cu pads after aging at 150°C for various time periods: (a) 100 h, (b) 300 h, (c) 700 h, and (d) 1000 h.

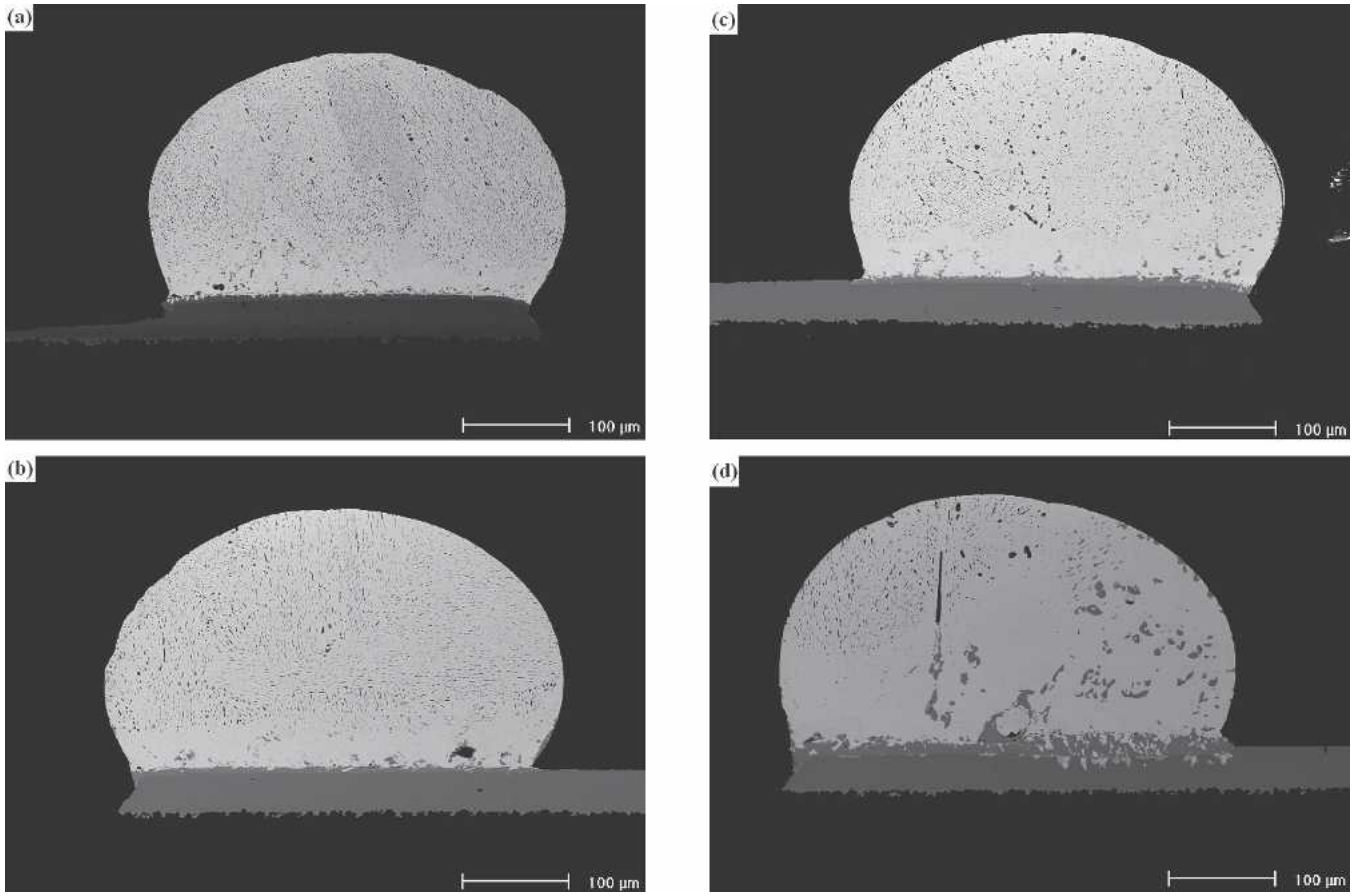

Fig. 10. Morphology of solder balls in Sn-9Zn BGA packages with Ag/Cu pads after aging at various temperatures and time periods: (a) 100°C, 300 h; (b) 100°C, 1000 h; (c) 150°C, 300 h; and (d) 150°C, 1000 h.

is Ag:Zn = 14.4:85.6, which corresponds to the ε-$AgZn_6$ phase in the Ag-Zn equilibria diagram. Figure 7 shows that the scallop-shaped ε-$AgZn_6$ intermetallic has not altered much after multiple reflows. However, an additional intermetallic layer has formed between the ε-$AgZn_6$ scallops and the Cu pad. The EDX analyses show that the composition (at.%) of the new intermetallic layer is in the γ-Cu_5Zn_8 phase.

The γ-Cu_5Zn_8 intermetallic layer also appears at the interface (Fig. 8a) after aging of the single-reflowed specimen at 100°C for 100 h. However, in Fig. 8a, the ε-$AgZn_6$ scallops are found to have detached from the γ-Cu_5Zn_8 intermetallic layer. Aged at 100°C for 300 h, the ε-$AgZn_6$ intermetallic scallops are observed (Fig. 8b) to have floated much farther away from the γ-Cu_5Zn_8 intermetallic layer. With further increases of the aging time, the ε-$AgZn_6$ intermetallic compounds are dispersed in the solder matrix, and the γ-Cu_5Zn_8 layer has grown, as revealed in Fig. 8b–d. In Fig. 8, depletion of the Zn-rich precipitates can also be observed in the solder region near the interfacial γ-Cu_5Zn_8 intermetallic layers. The result indicates that the growth of γ-Cu_5Zn_8 intermetallics is caused by the reaction between the Cu pad and the Zn atoms from the solder matrix. The exhaust of the Zn content in Sn-9Zn solder appears to have caused the dissolution of Zn-rich precipitates near the solder/pad interfaces.

After aging at 150°C, many γ-Cu_5Zn_8 intermetallic compounds are observed to strip off and float into the solder matrix of the Ag-surface finished Sn-9Zn BGA packages, as shown in Fig. 9. After prolonged aging for 1000 h, the thick γ-Cu_5Zn_8 intermetallic layer becomes porous, with the solder penetrated into the Cu pad in scallop form (Fig. 9d). The penetration of Sn-9Zn solder into the Cu pad can be easily observed in Fig. 10d, as compared to the morphology of the solder balls after aging under other conditions listed in Fig. 10.

The growth thickness of the γ-Cu_5Zn_8 intermetallic layer at the interfaces between the Sn-9Zn solder balls and the Cu pads after aging at 100°C and 150°C is plotted versus the square root of aging time. The linear relation in Fig. 11a implies that the growth kinetics of γ-Cu_5Zn_8 interfacial intermetallics is diffusion controlled. Since the source for Zn atoms in the growth of γ-Cu_5Zn_8 is the dissolution of Zn-rich precipitates in the solder matrix, the widths of the precipitate depletion regions at the aging temperatures of 100°C and 150°C are measured and plotted in Fig. 11b versus the square root of aging time. The linear relation of both curves indicates that the reaction is also diffusion controlled. The lattice diffusivities of Zn in Sn matrix at 100°C and

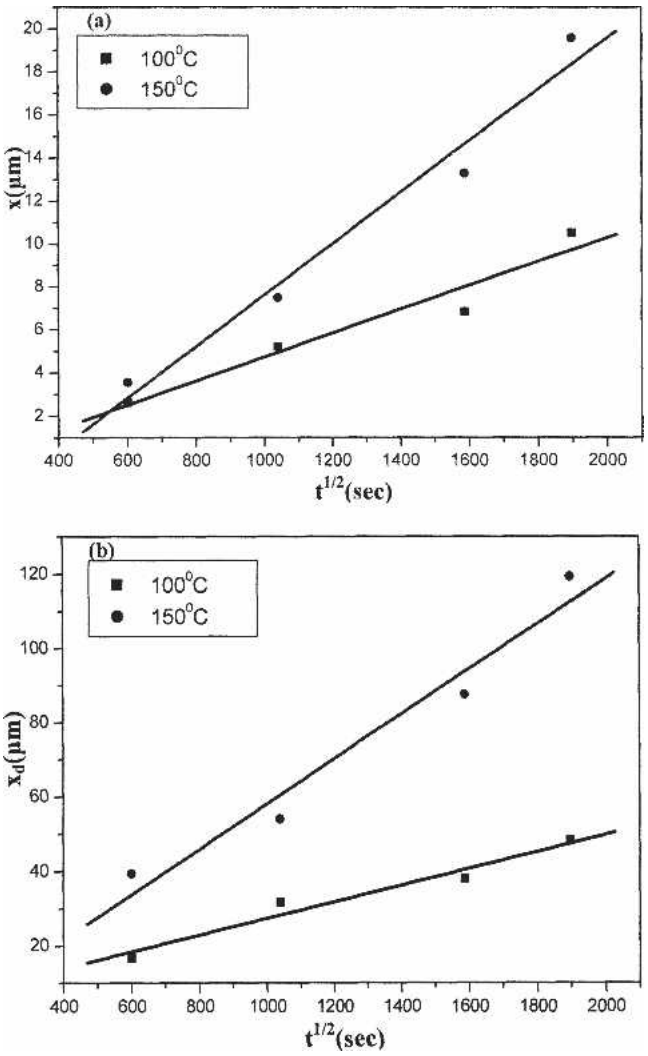

Fig. 11. Thickness (x) of the γ-Cu_5Zn_8 interfacial intermetallic layer and precipitate-free zone (x_d) in the solder matrix of immersion Ag surface finished Sn-9Zn BGA packages after aging at 100°C and 150°C relative to the square root of time ($t^{1/2}$).

150°C, as calculated from the equation of Huang and Huntington,[17]

$$D\ (m^2/s) = 1.1 \times 10^{-6} \exp\left(-\frac{50.2\ kJ/mol}{RT}\right),$$

are 1.01×10^{-13} m^2/s and 6.91×10^{-13} m^2/s. The diffusion distances ($d = \sqrt{Dt}$) at 100°C after aging times of 100 h and 1000 h are 191 μm and 650 μm, respectively. For the aging temperature of 150°C for 100 h and 1000 h, the diffusion distances of Zn atoms in Sn matrix are 499 μm and 1577 μm, respectively. In comparison with Fig. 11a, it is evidenced that the depletion widths of Zn-rich precipitates during the aging treatments are about tenfold smaller than the diffusion distances of Zn atoms in Sn matrix. Similar to the former case, the Au/Ni surface finished Sn-9Zn BGA packages, the results indicate that the controlled mechanism for the dissolution kinetics of Zn-rich precipitates in the Ag surface finished solder joints is the interfacial reaction between the Sn-9Zn solder and the Cu pad, rather than the lattice diffusion of Zn atoms through the solder matrix.

The ball shear strengths of solder joints in Sn-9Zn BGA packages with Au/Ni/Cu and Ag/Cu pads after various reflow and aging treatments are summarized in Table I. A single reflow cycle for Au/Ni surface finished packages results in a bonding strength of 8.6 N, which remains almost unchanged after multiple reflows, as shown in Fig. 12. For the Sn-9Zn solder joints with Ag/Cu pads, the bonding strength decreased slightly from the single reflowed condition (4.8 N) to the three times reflowed condition (4.3 N). The results also indicated that the reflowed Sn-9Zn solder BGA packages with Au/Ni/Cu pads possessed ball shear strengths twofold higher than those with Ag/Cu pads. Figure 13 compares the fractography of as-reflowed Au/Ni and Ag surface finished solder joints after the ball shear test. It is evidenced that the Sn-9Zn BGA packages with Au/Ni/Cu pads fractured along the solder matrix with a fully ductile characteristic (Fig. 13a). However, Fig. 13b and 13c demonstrate that the as-reflowed Ag surface finished Sn-9Zn packages after the ball shear test fractured along the solder/pad interface, with the exposure of the interfacial ε-$AgZn_6$ intermetallic layer (referring to Fig. 7a). It has been shown in Fig. 2 that the interface between the Sn-9Zn solder and the Ni/Cu pad after reflowing was free of intermetallic compounds. The much lower ball shear strength of the as-reflowed Ag surface finished Sn-9Zn packages, in comparison with those with the Au/Ni surface finish, should be attributed to the existence of brittle ε-$AgZn_6$ interfacial intermetallics in the former packages.

Aging at 100°C for 100 h causes the ball shear strengths of single reflowed Sn-9Zn packages with Au/Ni/Cu and Ag/Cu pads to decrease drastically to 7.2 N. With further increases of the aging time, the bonding strengths remain almost constant, as revealed in Fig. 13. The degradation of bonding strengths for both surface finished packages after aging at 150°C are similar to those of packages aged at 100°C. Fractography of all aged Sn-9Zn packages with Au/Ni/Cu and Ag/Cu pads after ball shear tests reveal a dimple characteristic (Fig. 15). The solder

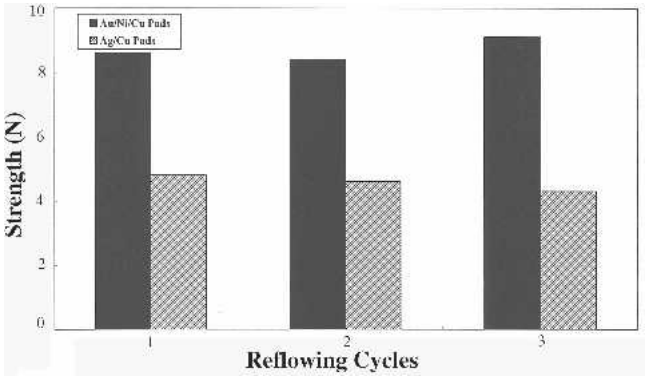

Fig. 12. Ball shear strengths of Sn-9Zn solder BGA packages with Au/Ni/Cu and Ag/Cu pads after various reflow cycles.

Table I. Ball Shear Strengths of the Sn-9Zn Solder BGA Packages with Au/Ni/Cu and Ag/Cu Pads after Various Reflow and Aging Treatments

Surface Finishing	Au/Ni/Cu Pads				Ag/Cu Pads			
Reflowing	**1 × Reflowing**		**2 × Reflowing**	**3 × Reflowing**	**1 × Reflowing**		**2 × Reflowing**	**3 × Reflowing**
Aging	**100°C**	**150°C**			**100°C**	**150°C**		
0	8.6N	8.6N	8.4N	9.1N	4.8N	4.8N	4.6N	4.3N
100 h	7.2N	7.2N	—	—	3.2N	2.9N	—	—
300 h	7.4N	7.5N	—	—	3.1N	2.7N	—	—
500 h	7.0N	7.3N	—	—	2.9N	2.5N	—	—
700 h	7.5N	7.4N	—	—	2.6N	2.5N	—	—
1000 h	7.0N	7.0N	—	—	2.7N	2.4N	—	—

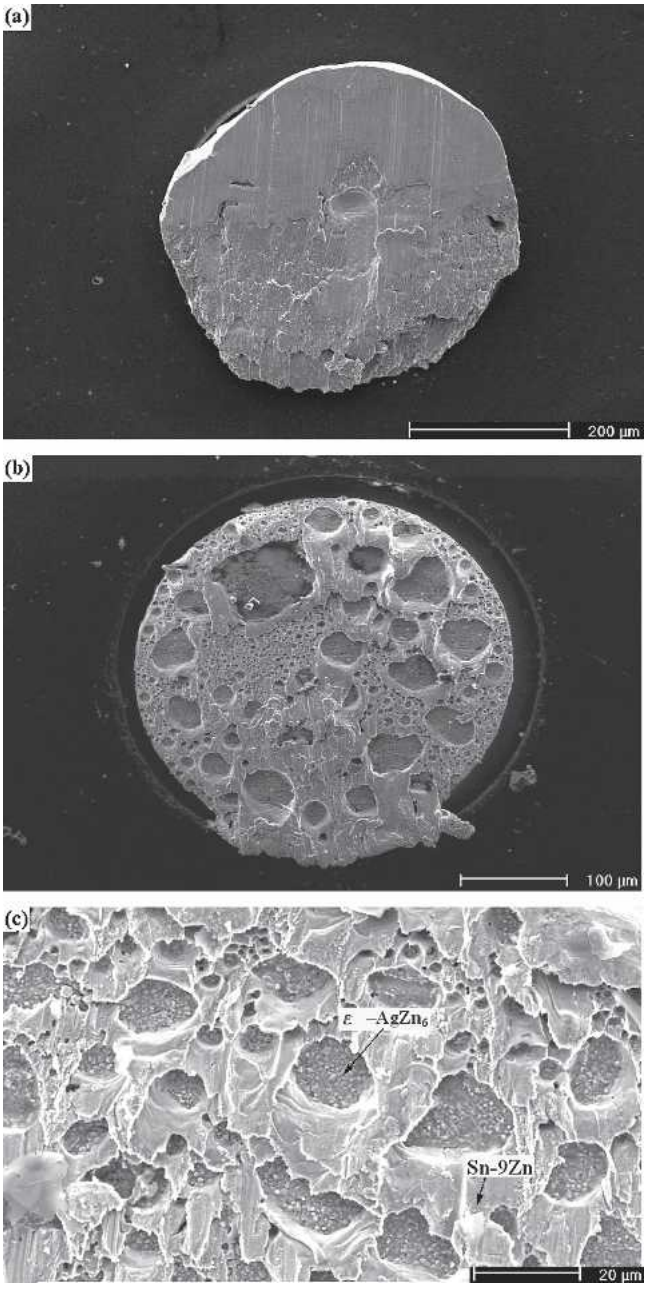

Fig. 13. Fractography of solder joints after ball shear tests in the as-reflowed Sn-9Zn BGA packages with various surface finishes: (a) Au/Ni/Cu pads and (b) and (c) Ag/Cu pads.

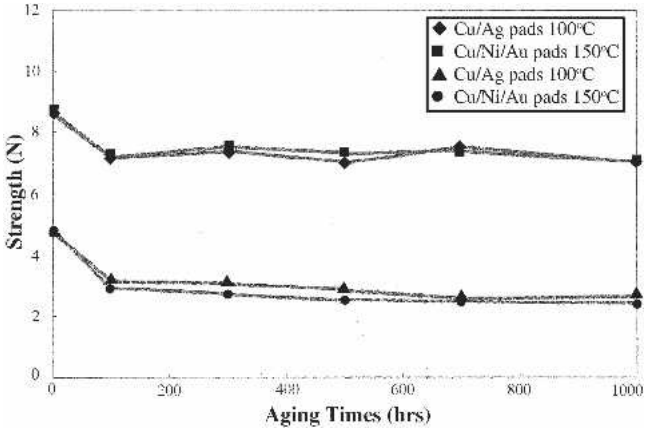

Fig. 14. Ball shear strengths of Sn-9Zn solder BGA packages with Au/Ni/Cu and Ag/Cu pads after aging at 100°C and 150°C for various times.

joints have fractured along the solder matrix for those aged at either 100°C or 150°C. The result implies that the appearance of the $Ni_4Zn_{21}$and γ-Cu_5Zn_8 intermetallic layers at the solder/pad interface of Au/Ni and Ag surface finished Sn-9Zn packages after aging at 150°C has not affected the bonding strength. To elucidate the degradation of bonding strengths in the aged solder joints, the hardness of the solder balls is measured and shown in Fig. 16. It is obvious that both tendencies of the ball strength (Fig. 14) and solder ball hardness (Fig. 16) are quite consistently related to the aging time. The results indicate that the strength degradation of solder joints in both surface finished packages after aging is caused by the softening of the solder matrix. The softening effect of Sn-9Zn solder balls with Au/Ni/Cu pads after aging is attributed to the depletion of Zn-rich precipitates in both solder matrices due to the growth of the Ni_4Zn_{21} and γ-Cu_5Zn_8 intermetallic layers, respectively. However, the depletion zones of Zn-rich precipitates due to the formation and growth of the Ni_4Zn_{21} intermetallic layer in the Au/Ni surface finished packages after aging are much narrower than those for Sn-9Zn solder joints with Ag/Cu pads. From Fig. 14, the decrease in bonding strengths of Au/Ni and Ag surface finished Sn0-9Zn packages after aging processes are about 17% and 40%, respectively. The much more severe degrada-

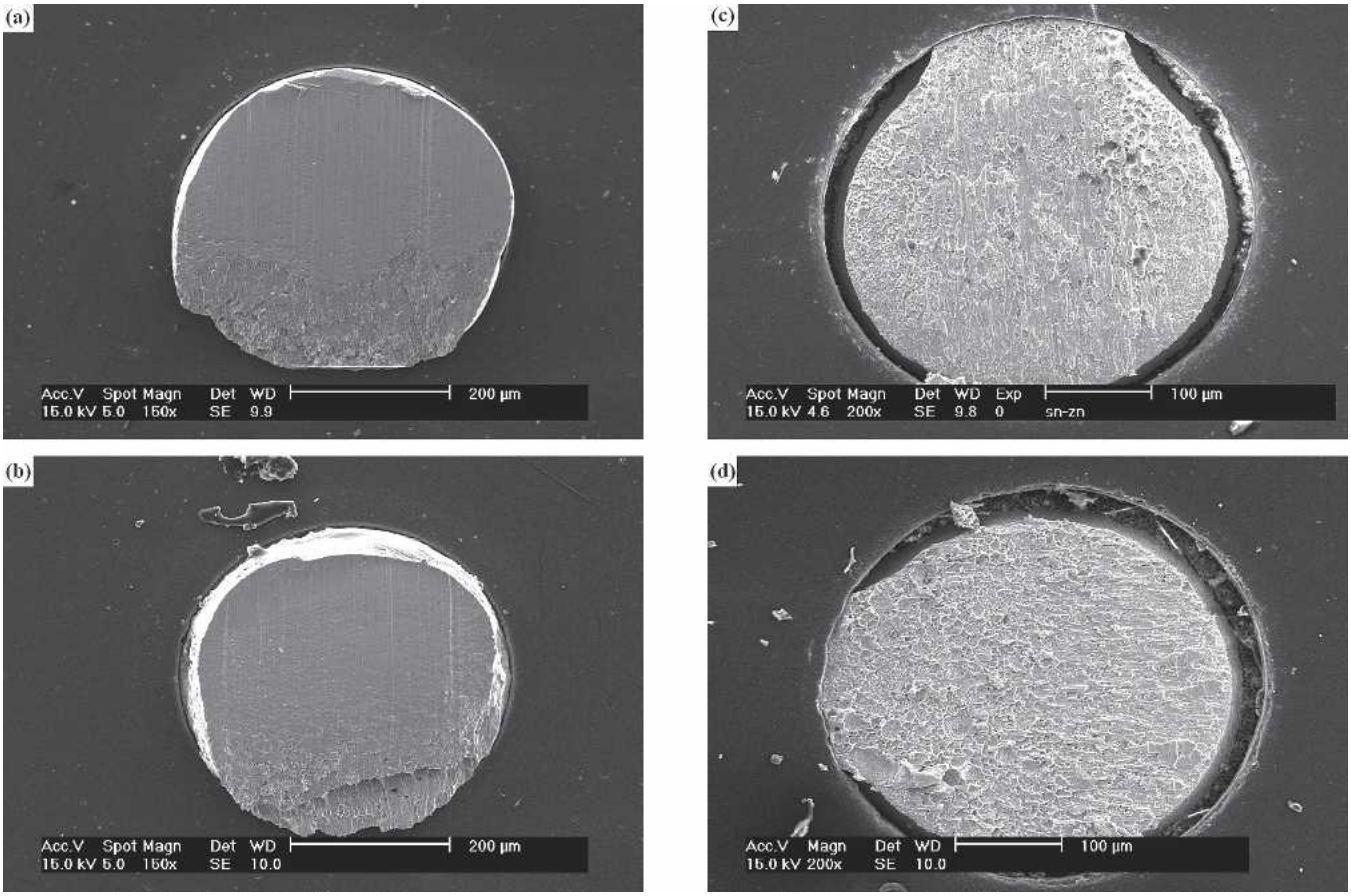

Fig. 15. Typical fractography of ball shear tested solder joints in Sn-9Zn BGA packages with Au/Ni/Cu and Ag/Cu pads after aging at various temperatures: (a) Au/Ni/Cu pads, 100°C aging; (b) Au/Ni/Cu pads, 150°C aging; (c) Ag/Cu pads, 100°C aging; and (d) Ag/Cu pads, 150°C aging.

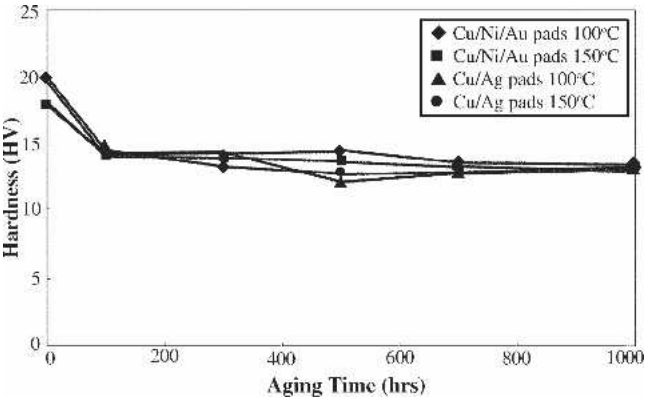

Fig. 16. Hardness of solder balls in Sn-9Zn BGA packages with Au/Ni/Cu and Ag/Cu pads after aging at 100°C and 150°C for various times.

tion of aged solder joints in Sn-9Zn BGA packages with Ag/Cu pads in comparison to those with Au/Ni/Cu pads is consistent with the wider precipitate-free zones in the former case, which can be attributed to the higher growth rate of Cu-Zn intermetallics than Ni-Zn intermetallics at the solder/pad interfaces.[11]

CONCLUSIONS

The intermetallic compounds formed in Sn-9Zn solder joints of BGA packages with Au/Ni/Cu and Ag/Cu pads after the reflow and aging processes are investigated. Experimental results show that the Au and Ag thin film dissolves rapidly during reflow and reacts with the Zn atoms of Zn-rich precipitates embedded in the Sn-9Zn solder matrix to form a γ_3-$AuZn_4$/γ-Au_7Zn_{18} intermetallic double layer and ε-$AgZn_6$ intermetallic scallops, respectively. Multiple reflows cause the γ_3/γ intermetallics in the Au/Ni-surface finished Sn-9Zn packages to float away from the Ni/Cu pads. After aging at 100°C and 150°C, γ_3-$AuZn_4$ grows as a result of the reaction between γ-Au_7Zn_{18} and the Zn atoms dissolved from Zn-rich precipitates near the γ_3/γ layer. At the interface between the Sn-9Zn solder and the Ni/Cu pad, an additional Ni_4Zn_{21} intermetallic layer appears at the aging temperature of 150°C. For the immersion Ag surface finished Sn-9Zn BGA packages, it was observed that multicycle reflows caused an additional γ-Cu_5Zn_8 intermetallic layer to form between ε-$AgZn_6$ scallops and the Cu pad. γ-Cu_5Zn_8 intermetallics also appeared after the aging of the reflowed specimens at 100°C and 150°C. However, the ε-$AgZn_6$ scallops were found to detach from the γ-Cu_5Zn_8 intermetallic layer and float into the solder matrix. The growth of Ni_4Zn_{21} and γ-Cu_5Zn_8 interfacial intermetallics causes the depletion of Zn-rich precipitates in the solder ball near the solder/pad interfaces. Ball shear testing revealed that the as-reflowed Sn-9Zn BGA solder joints with Au/Ni/Cu

and Ag/Cu pads possessed bonding strengths of 8.6 N and 4.8 N, respectively. The depletion of Zn-rich precipitates near the solder/pad interfaces after the aging process accounts for the softening effect of the solder matrix. This resulted in degradation of the ball shear strength of Au/Ni and Ag surface finished Sn-9Zn packages by about 17% and 40%, respectively.

ACKNOWLEDGEMENT

The authors gratefully acknowledge the financial support from the National Science Council, Taiwan, for this study under Grant No. 93-2216-E002-024.

REFERENCES

1. N.C. Lee, *Adv. Microelectron.* 26, 29 (1999).
2. H.J. Lau, C.P. Wong, N.C. Lee, and S.W. Ricky Lee, *Electronics Manufacturing with Lead-Free, Halogen-Free & Conductive-Adhesive Materials* (New York: McGraw-Hill Handbooks, 2003).
3. Z. Chen, M. He, and G. Qi, *J. Electron. Mater.* 33, 1465 (2004).
4. J.W. Yoon, S.W. Kim, and S.B. Jung, *J. Alloys Compounds* 391, 82 (2005).
5. M.Y. Chiu, S.Y. Chang, Y.H. Tseng, Y.C. Chan, and T.H. Chuang, *Z. Metallkd.* 93, 248 (2002).
6. Y.C. Chan, M.Y. Chiu, and T.H. Chuang, *Z. Metallkd.* 93, 95 (2002).
7. M.Y. Chiu, S.S. Wang, and T.H. Chuang, *J. Electron. Mater.* 31, 494 (2002).
8. P. Harris, *Soldering Surf. Mount Technol.* 11, 46 (1999).
9. R.K. Shiue, L.W. Tsay, C.L. Lin, and J.L. On, *Microelectron. Reliab.* 43, 453 (2003).
10. T.H. Chuang, H.M. Wu, M.D. Cheng, S.Y. Chang, and S.F. Yen, *J. Electron. Mater.* 33, 22 (2004).
11. Y.C. Chan, M.Y. Chiu, and T.H. Chuang, *Z. Metallkd.* 93, 95 (2002).
12. K. Suganuma and K. Niihara, *J. Mater. Res.* 13, 2859 (1998).
13. W.H. Lin and T.H. Chuang, *Mater. Eng. Performance* 12, 452 (2003).
14. H.M. Lee, S.W. Yoon, and B.J. Lee, *J. Electron. Mater.* 27, 1161 (1998).
15. S.W. Yoon, J.R. Soh, H.M. Lee, and B.J. Lee, *Acta Mater.* 45, 951 (1997).
16. S.W. Yoon, W.K. Choi, and H.M. Lee, *Scripta Mater.* 40, 327 (1999).
17. F.H. Huang and H.B. Huntington, *Phys. Rev.* B9 1479 (1974).